# Nonequilibrium phase transition and self-organized criticality in a sandpile model with stochastic dynamics

S. Lübeck,[1,*] B. Tadić,[2,†] and K. D. Usadel[1,‡]

[1] *Theoretische Tieftemperaturphysik, Gerhard-Mercator-Universität Duisburg, Lotharstrasse 1, 47048 Duisburg, Germany*
[2] *Jožef Stefan Institute, University of Ljubljana, P.O. Box 100, 61111 Ljubljana, Slovenia*
(Received 14 September 1995)

We introduce and study numerically a directed two-dimensional sandpile automaton with probabilistic toppling (probability parameter $p$), which provides a good laboratory to study both self-organized criticality and the far-from-equilibrium phase transition. In the limit $p = 1$ our model reduces to the critical height model in which the self-organized critical behavior was found by exact solution [D. Dhar and R. Ramaswamy, Phys. Rev. Lett. **63**, 1659 (1989)]. For $0 < p < 1$ metastable columns of sand may be formed, which are relaxed when one of the local slopes exceeds a critical value $\sigma_c$. By varying the probability of toppling $p$ we find that a continuous phase transition occurs at the critical probability $p_c$, at which the steady states with zero average slope (above $p_c$) are replaced by states characterized by a finite average slope (below $p_c$). We study this phase transition in detail by introducing an appropriate order parameter and the order-parameter susceptibility $\chi$. In a certain range of $p < 1$ we find the self-organized critical behavior that is characterized by nonuniversal $p$-dependent scaling exponents for the probability distributions of size and length of avalanches. We also calculate the anisotropy exponent $\zeta$ and the fractal dimension $d_f$ of relaxation clusters in the entire range of values of the toppling parameter $p$. We show that the relaxation clusters in our model are anisotropic and can be described as fractals for values of $p$ above the transition point. Below the transition they are isotropic and compact.

PACS number(s): 05.40.+j

## I. INTRODUCTION

The term "self-organized criticality" (SOC) [1] refers to certain driven dissipative systems which organize themselves into a steady state far away from equilibrium. The critical steady state appears as an attractor of the dynamics, and thus no fine tuning of an external parameter is necessary to achieve criticality. The major aspect of the dynamics of SOC systems is the "separation of time scales," i.e., the system relaxes infinitely fast compared to the time between two successive perturbations. From this point of view the relaxation processes may be considered as consisting of a series of discrete events (avalanches) and one investigates the probability distribution of their spatial properties, for instance, the size of an avalanche. The self-organized critical state is characterized by a power-law behavior of these probability distributions. For detailed discussions of the definition of SOC we refer to [2,3].

Sandpile automata [1,4,5] are well known prototype models exhibiting SOC. By adding a particle from the outside, a sandpile is perturbed and the perturbation may lead to instabilities at neighboring sites if the local height of sand exceeds a critical value $h_c$ [critical height

model (CHM) [1,4]], or if the local slopes exceed a critical value $\sigma_c$ [critical slope model (CSM) [5–7]]. The steady state of the system in the case of the CHM is accompanied by a state of a zero average slope. A finite average slope characterizes a CSM.

In Sec. II we introduce a two dimensional directed sandpile model with stochastic dynamics, in which the updating rules may be tuned continuously by varying a parameter $p$, representing probability of toppling, between the CHM (for $p = 1$) and the CSM (for $p = 0$) [8]. Our numerical results for $p < 1$ show that a nonequilibrium phase transition takes place at the critical value $p_c$, which is characterized by a continuous appearance of a nonzero average slope below the critical point. In order to characterize this phase transition quantitatively, we introduce an order parameter $\langle \sigma \rangle$, representing the net average slope. Results obtained from numerical simulations of the order parameter $\langle \sigma \rangle$, as well as the order parameter susceptibility and the penetration depth of the slope, will be given in Sec. III.

We also study fractal properties of the avalanches by calculating their fractal dimension in the entire range of values of the parameter $p$ (Sec. IV). Our results suggest that for values of $p$ above the transition point the avalanches can be described as self-affine fractals, i.e., the shape of the avalanches exhibits anisotropic behavior. Below the transition point both properties, the fractality and anisotropy of the relaxation clusters, are lost.

In Sec. V we present a detailed analysis of the probability distributions of the avalanches and address the question of whether the model exhibits SOC for $p < 1$.

---

*Electronic address: sven@hal6000.thp.uni-duisburg.de
†Electronic address: Bosiljka.Tadic@ijs.si
‡Electronic address: usadel@hal6000.thp.uni-duisburg.de

A finite size scaling analysis of the probability distributions and a check of certain scaling equations yielded that the model displays SOC for certain values of $p < 1$.

## II. MODEL

We consider a two-dimensional sandpile model on a square lattice of size $L \times L$ and integer variables $h(i,j)$ representing the local height. We assume a directed dynamics, i.e., particles are restricted to flow in the downward direction (increasing $i$). According to the widespread "sandpile language," the first row ($i = 1$) and the last row ($i = L$) represent the top and the bottom of the pile, respectively. To minimize the influence of the horizontal boundaries we limit our investigations to periodic boundary conditions in this horizontal direction ($j$ direction). Any site of the lattice has two downward and two upward next neighbors, namely, $h(i+1, j_\pm)$ and $h(i-1, j_\pm)$ with $j_\pm = j \pm \frac{1}{2}[1 \pm (-1)^i]$.

We perturb the system by adding particles at a random place on the top of the pile according to

$$h(1,j) \mapsto h(1,j) + 1 \qquad \text{with random } j. \qquad (1)$$

A site is called unstable if the height $h(i,j)$ or at least one of the two slopes

$$\sigma(i, j_\pm) = h(i,j) - h(i+1, j_\pm) \qquad (2)$$

exceeds its respective critical value, i.e., if $h(i,j) \geq h_c$ or $\sigma(i, j_\pm) \geq \sigma_c$.

If both slopes are critical one particle after another drops alternately to the next downward neighbors until both slopes become subcritical. In the case that one slope exceeds $\sigma_c$ particles drop to the corresponding downward neighbor.

In contrast to the critical slope, the critical height condition has a stochastic character. If the local height exceeds the critical value $h_c$ toppling occurs only with the probability $p$, and then two particles drop to the two downward neighbors.

Because each relaxing cell changes the heights or slopes of its four neighboring sites, the stability conditions are applied at these four activated sites in the next updating step. Toppling may take place after adding a particle on the first row. We apply the slope and the height stability conditions simultaneously for all activated sites. An avalanche stops if all activated sites are stable. Then we start again according to Eq. (1).

It should be emphasized that, in addition to the instability criteria, a site is considered as potentially unstable *only* when a particle drops at or near the site. Owing to the probabilistic character of the critical height toppling rule, locally heights could remain above critical after one relaxation event. In this respect, the present model for $0 < p < 1$ is different from already known critical height [1,4,5] and critical slope [5,6] models.

One can interpret the parameter $1-p$ as being due to static friction between the sand grains, which prevents toppling even if the height exceeds the critical value. In the case $p = 1$, our model is identical to the model of Dhar and Ramaswamy [4], which exhibits a robust SOC behavior. In the limit $p = 0$, our directed rules lead to a steady state where all slopes are equal, i.e., $\sigma(i, j_\pm) = \sigma_c - 1$. Thus, if a particle is added at the first row, it performs a directed random walk down the pile until it reaches the boundary and drops out of the system — no SOC can occur in this limit.

We fix the critical height $h_c$ and the critical slope $\sigma_c$ and restrict ourselves to $h_c = 2$ and $\sigma_c = 8$, although it should be emphasized that the results depend on the choice of these parameters.

The behavior of our model is characterized by anisotropy effects caused by the preferred direction of the assumed dynamics. This anisotropy may influence, for instance, the fractal properties of the avalanches. If a measured quantity depends on the direction we introduce in these cases two different values which describe the behavior in the parallel and perpendicular directions, respectively, e.g., the fractal dimensions $d_\parallel$ and $d_\perp$. The parallel direction corresponds to the preferred direction of the dynamics (increasing $i$).

## III. NONEQUILIBRIUM PHASE TRANSITION

In this section we consider the general behavior of the system, i.e., how the transition from the CHM to the CSM takes place. As mentioned above a CHM is characterized by a zero average slope in contrast to a CSM where the steady state displays a nonzero average slope. In order to describe this transition quantitatively, we introduce as an order-parameter the mean slope of the system [8]:

$$\langle \sigma \rangle = \left\langle \frac{1}{L_\parallel L_\perp} \sum_{i,j} \sigma_{ij} \right\rangle , \qquad (3)$$

where $\langle \rangle$ stands for the average over the total number of events and $\sigma_{ij}$ is the local slope at site $(i,j)$, which is defined as

$$\sigma_{ij} = \frac{1}{2}(2h_{i,j} - h_{i+1,j_+} - h_{i+1,j_-}). \qquad (4)$$

The summation in Eq. (3) runs from $j = 1, 2, 3, \ldots, L$ in the perpendicular direction, and from $i = 21, 22, \ldots, L - 20$ in the parallel direction, in order to suppress the boundary effects from the first and last rows of the system. Of course the results obtained are independent of the value of the cutoff length, provided that it is large enough. To normalize the order-parameter one has to choose $L_\parallel = L - 40$ and $L_\perp = L$. The nature of the transition as well as the transition point $p_c$ should be determined from the $p$ dependence of the average slope Eq. (3) in the vicinity of $p_c$.

In Fig. 1 we show the results of numerical simulations of the order-parameter defined in Eq. (3). The order-parameter vanishes at the transition point, i.e.,

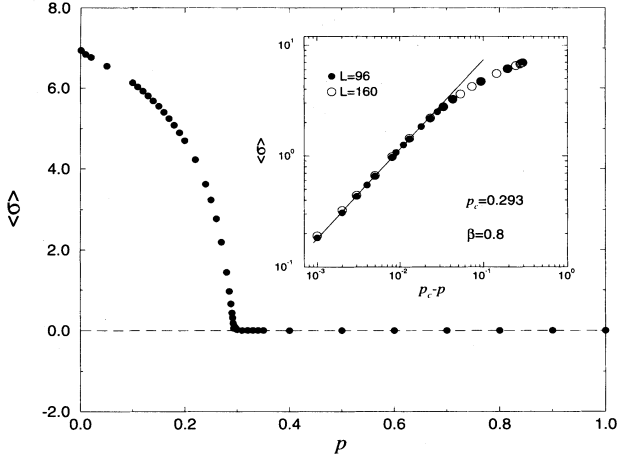$$\langle \sigma \rangle \sim (p_c - p)^\beta, \qquad (5)$$

FIG. 1. Average slope of the pile $\langle\sigma\rangle$ plotted vs probability $p$. The solid line inside the inset corresponds to a fit according to Eq. (3).



FIG. 2. The $p$ dependence of the order-parameter susceptibility for different system sizes $L$. The inset displays the scaling behavior of the height regime. The solid line corresponds to a power law with exponent $\gamma = 0.98$.

as one can see from the inset of Fig. 1. We determine the transition point $p_c = 0.293 \pm 0.002$ and the exponent $\beta = 0.8 \pm 0.05$ for automaton sizes $L = 64, 96, 128, 160$, and 192.

We next analyze the fluctuation of the order parameter. An ordering susceptibility can be defined as [9]

$$\chi = L_\parallel L_\perp \ (\langle\sigma^2\rangle - \langle\sigma\rangle^2). \tag{6}$$

Unfortunately the average slope has a self-averaging character in the critical height regime, which means $\chi$ vanishes for $L \to \infty$ due to a cancellation of the correlations $\langle\sigma_{ij}\sigma_{kl}\rangle$ in the interior of the pile. Consequently the susceptibility depends only on the boundary term and is of relative magnitude $\sim L_\parallel^{-1}$. In the case $p = 1$ the order-parameter susceptibility can be calculated exactly and is given by

$$\chi = \frac{1}{2L_\parallel}. \tag{7}$$

In Fig. 2 we display the susceptibility $\chi$ for varying $p$ and four different automata sizes. For all considered automata sizes $\chi$ is sharply peaked at the transition point $p_c = 0.293$.

In the inset of Fig. 2 we plot $\chi L_\parallel$ vs $p$. All different curves collapse, except for the values which are close to the transition point. The susceptibility scales as

$$\chi \sim L_\parallel^{-1}(p - p_c)^{-\gamma} \tag{8}$$

with $\gamma = 0.98 \pm 0.05$. One can see from Fig. 2 that this power-law behavior of $\chi$ holds away from $p_c$ up to a certain cutoff value which tends to $p_c$ if $L \to \infty$. Due to this $L$ dependence the order-parameter susceptibility tends to zero with increasing $L$ for $p > p_c$.
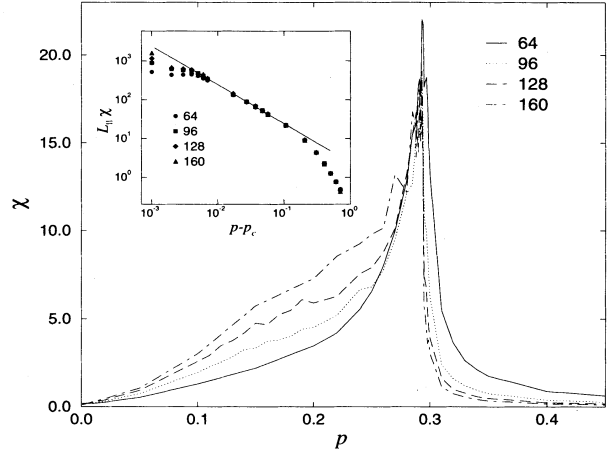
Below the critical point our data suggest that the sus-

ceptibility displays a complicated scaling behavior (see Fig. 2). It is still an open question whether $\chi$ diverges with increasing system size $L$ or converges to a finite, i.e., $L$-independent, value. To address this question one has to simulate extremely large systems which is beyond our present computer capacity.

In order to break off the self-averaging character of the average slopes we defined a nonlinear susceptibility

$$\chi_{nl} = L_\parallel L_\perp \ (\langle\sigma_{nl}^2\rangle - \langle\sigma_{nl}\rangle^2) \tag{9}$$

with

$$\sigma_{nl} = \frac{1}{L_\parallel L_\perp} \sum_{i,j} \sigma_{ij}^2. \tag{10}$$

We found that $\chi_{nl}$ shows a cusp at $p_c$, i.e., the nonlinear susceptibility is independent of $L$ in both regimes (not shown). This behavior is consistent with the exact value for $p = 1$:

$$\chi_{nl} = \frac{9}{64} + O(L^{-1}). \tag{11}$$

The nondiverging behavior of the susceptibilities indicates that the nonequilibrium phase transition is not characterized by a diverging correlation length. Thus we address the question of how the finite slope occurs by approaching the transition point. In Fig. 3 we display the average height profile $\langle h\rangle(i)$ of the pile for certain values of $p$. For $p < 1$ a finite slope occurs at the boundaries and the pile grows up from the bottom of the pile. The slopes penetrate the hole system from the edge of the automaton. We determine the penetration depth $\lambda$ of the slopes by measuring the distance of the profile maximum from the right boundary (see Fig. 3). The results obtained are plotted in the inset of Fig. 3 for automaton sizes $L = 100$ and 200. Close to the transition point the penetration
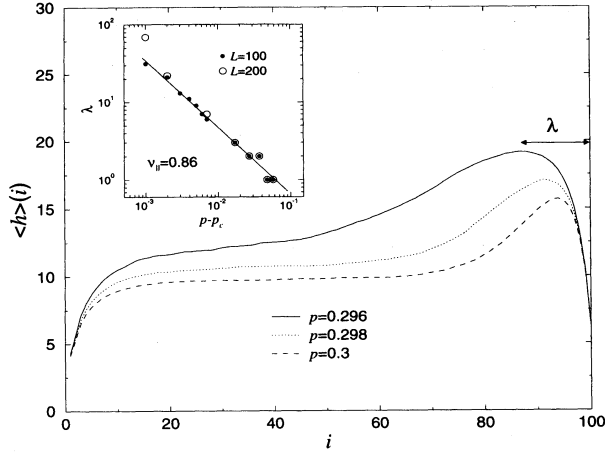
FIG. 3. The average height profile $\langle h(i) \rangle$ along the parallel direction. The penetration depth $\lambda$ is determined as the distance from the maximum height to the right boundary of the system. The inset displays the $p$ dependence of $\lambda$.

depth obeys a power-law behavior like

$$\lambda \sim (p - p_c)^{-\nu_{\parallel}} . \tag{12}$$

Our numerical analysis yielded $\nu_{\parallel} = 0.86 \pm 0.06$.

## IV. FRACTAL PROPERTIES OF THE AVALANCHES

In this section we consider the scaling properties of the avalanches. We define the size $s$ of the avalanches as the number of toppled sites in one event. The length of an avalanche is defined as the distance from the first row to the toppled site with maximal value of the index $i$. Note that this length is by definition parallel to the preferred direction, and will be denoted as $l_{\parallel}$. We introduce the average width $l_{\perp}$ of an avalanche via

$$l_{\perp} = \left( l_{\parallel}^{-1} \sum_{i=1}^{l_{\parallel}} l_{\perp}(i)^q \right)^{\frac{1}{q}} , \tag{13}$$

where $l_{\perp}(i)$ is the width of an avalanche in the $i$th row. Since there is some arbitrariness in the definition of $l_{\perp}$ we tried both $q = 1$ and $q = 2$ with the result that the scaling properties of the width are practically the same in both cases. For the sake of simplicity we present in this paper only the results for $q = 2$. We assume that the size of avalanches is scale invariant with both the length and width. In order to take the anisotropy of avalanches into account, we introduce two different scaling exponents $d_{\parallel}$ and $d_{\perp}$, corresponding to different directions of scaling $l_{\parallel}$ and $l_{\perp}$, respectively [10,11]. We assume that the average size $\langle s \rangle$ of all avalanches of length $l_{\parallel}$ and of width $l_{\perp}$, respectively, scales as

$$\langle s \rangle_{l_{\parallel}} \sim l_{\parallel}^{d_{\parallel}} \quad \text{and} \quad \langle s \rangle_{l_{\perp}} \sim l_{\perp}^{d_{\perp}} . \tag{14}$$

If both scaling relations are valid the width scales with the length as

$$l_{\perp} \sim l_{\parallel}^{\zeta} \quad \text{with} \quad \zeta = \frac{d_{\parallel}}{d_{\perp}}, \tag{15}$$

where the exponent $\zeta$ describes the anisotropic behavior of the avalanches. Since there are only two independent exponents we measured $d_{\parallel}$ and $\zeta$ according to Eq. (13)–Eq. (15).

We find that with decreasing $p$ the parallel fractal dimension $d_{\parallel}$ increases from the exactly known value $d_{\parallel} = \frac{3}{2}$ in the limit $p = 1$ to 2 at the transition point. In the critical slope regime $d_{\parallel}$ remains constant and $d_{\parallel} = 2$ [8].

Figure 4 shows how the width depends on the length for different values of $p$. In all cases we found that Eq. (15) is valid and extracted values of the anisotropy exponent $\zeta$ (see the inset to Fig. 4). With decreasing $p$ the anisotropy exponent $\zeta$ increases from $\zeta = \frac{1}{2}$ at $p = 1$ and reaches its maximum value $\zeta \simeq 1$ for $p \leq p_c$. We expect that this expression is exactly given by $\zeta = 1$ and that the observed deviations in the critical slope regime are caused by finite size effects. The origin of the huge error bars for $p < p_c$ is a finite curvature of the corresponding curves in the log-log plots. These curvatures would be reduced by studying larger systems, leading eventually to the result $\zeta = 1$ with higher accuracy. Thus the critical height regime is characterized by an anisotropic shape of the avalanches ($\zeta < 1$). This behavior changes to an isotropic shape ($\zeta = 1$) on approaching the transition point. Due to the dependence of the scaling factors on the directions the avalanches can be regarded as an example of self-affine fractals. In analogy to self-similar fractals, it is possible to describe self-affine fractals by
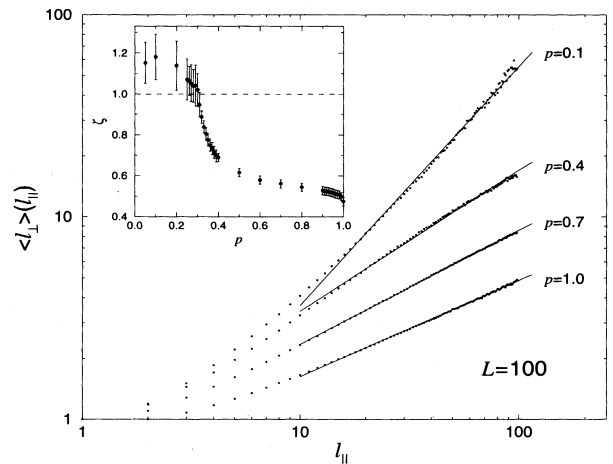


FIG. 4. Double logarithmic plot of the average width vs length for various values of $p$ as indicated. All curves obey a power-law behavior (solid lines) with different accuracy. The inset displays the $p$ dependence of the anisotropic exponent $\zeta$ obtained from the fits according to Eq. (15).

the single exponent $d_f$ given by [11]

$$d_f = 2\frac{d_{\parallel}}{\zeta + 1}. \qquad (16)$$

In Fig. 5 we show the results for the fractal dimension $d_f$ versus $p$ in the critical height regime. As seen from Fig. 5, the relaxation clusters exhibit a fractal behavior $(d_f < 2)$ in the critical height regime $p > p_c$, with the exception of the case $p = 1$. Although the deviation from $d_f = 2$ is very small it cannot be explained by statistical fluctuations due to the size of the error bars and the systematic character of the deviations from 2. Below the transition point, i.e., for $p < p_c$, the fractal dimension $d_f = 2$, corresponding to compact clusters.

One can easily explain this behavior by considering the shapes of the avalanches (see Fig. 4 in [8]). In the pure critical height model ($p = 1$) the avalanches are compact, i.e., no holes can occur in this limit. With decreasing $p$ some supercritical sites may remain in the interior of the avalanche due to the stochastic character of the dynamics, leading to holes and branching processes. This results in a fractal character of the avalanches. On approaching the transition point $p_c$ this structure of the avalanches is lost. In this region the dynamics is more and more characterized by toppling processes due to the critical slope condition. The slope between a toppled site and its two backward neighbors may exceed the critical value and toppling occurs again. Owing to these multiple topplings the probability to find holes inside an avalanche decreases with decreasing $p$ and eventually vanishes at $p_c$. At the same time branching of the relaxation clusters become rarer.

In this way, we may conclude that the phase transition from the critical height to the critical slope regime is accompanied by continuous change from fractal avalanches with an anisotropic shape above $p_c$ to compact and isotropic avalanches below $p_c$.
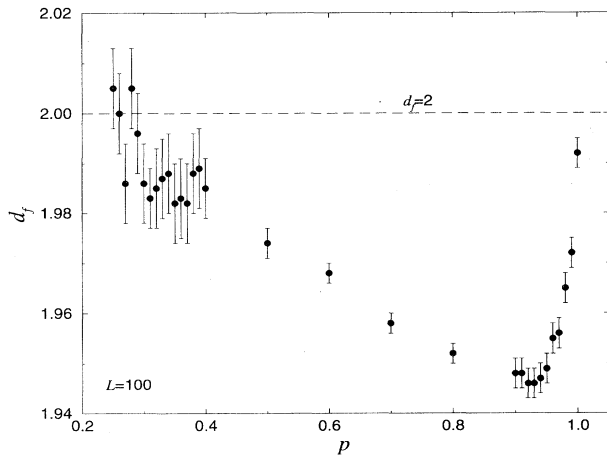
## V. AVALANCHE DISTRIBUTIONS

In this section we examine how the SOC behavior of the Dhar and Ramaswamy model vanishes with decreasing $p$. In the critical state, due to the absence of a characteristic length scale, the probability $P(l_{\parallel})$ for an avalanche longer than a certain length $l_{\parallel}$ obeys a power law, i.e.,

$$P(l_{\parallel}) \sim l_{\parallel}^{-\kappa}. \qquad (17)$$

Similarly, the probability distribution of an avalanche size larger than $s$ exhibits a power law with another exponent via

$$P(s) \sim s^{-\tau}, \qquad (18)$$

where $s$ is the number of different sites that relaxed in one event. Multiply relaxed sites are counted only once in this distribution. Double logarithmic plots of the distributions $P(l_{\parallel})$ and $P(s)$ for various values of the parameter $p$ and $L = 200$ are shown in Fig. 6 and Fig. 7.

One can see from Fig. 6 that the probability distribution $P(l_{\parallel})$ displays no cutoff in the critical height regime. For $p < p_c$ a sharp cutoff length occurs in the distribution $P(l_{\parallel})$. The dynamics is now dominated by the toppling processes due to the critical slope condition and thus the edge of the system ($i = L$) influences the topplings at a certain number of rows close to the edge. This behavior is typical for critical slope models.

Power-law behavior according to Eq. (17) and Eq. (18) occurs only in the critical height regime. The critical exponents $\kappa$ and $\tau$ are determined by the slopes of the linear sections of these curves for $p \geq 0.5$. For lower values of $p$ we found a finite curvature in the log-log plots of the distributions, indicating that the power-law behavior is lost for a range of values of $p$ preceding the transition point $p_c$. The obtained values of the exponents for certain values of $p$ are shown in Fig. 8 and are listed in Table I.



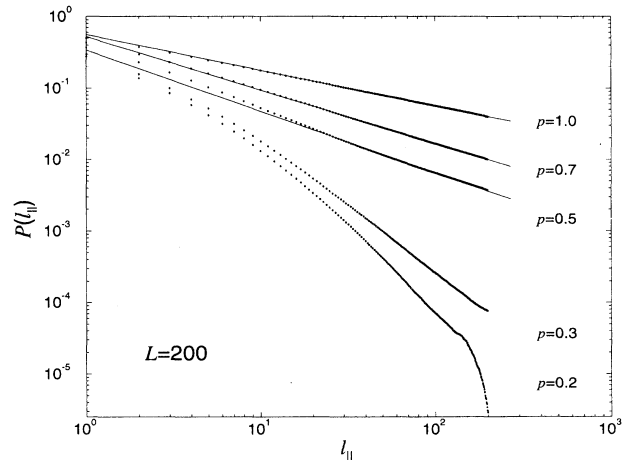FIG. 5. Fractal dimension $d_f$ of the avalanches for various values of $p$.



FIG. 6. Double logarithmic plot of the probability distribution $P(l_{\parallel})$ of avalanches of length $l_{\parallel}$ for various values of $p$ as indicated. The solid lines correspond to power laws.

TABLE I. The exponents for different values of toppling parameter $p$. Due to a lack of a power-law behavior of the corresponding quantities the exponents $\tau, \kappa$, and $\theta$ are not defined for $p < 0.5$.

| $p$ | $d_\|$ | $\zeta$ | $z$ | $\tau$ | $\kappa$ | $\theta$ |
|-----|--------|---------|-----|--------|----------|----------|
| 1.0 | 1.47 | 0.48 | 1.00 | 0.34 | 0.50 | 0.51 |
| 0.9 | 1.49 | 0.53 | 1.03 | 0.46 | 0.68 | 0.61 |
| 0.8 | 1.51 | 0.55 | 1.06 | 0.47 | 0.72 | 0.65 |
| 0.7 | 1.53 | 0.56 | 1.10 | 0.49 | 0.75 | 0.67 |
| 0.6 | 1.56 | 0.58 | 1.15 | 0.53 | 0.79 | 0.69 |
| 0.5 | 1.60 | 0.62 | 1.21 | 0.58 | 0.86 | 0.75 |
| 0.4 | 1.68 | 0.69 | 1.33 | | | |
| 0.3 | 2.01 | 1.02 | 1.70 | | | |
| 0.2 | 2.11 | 1.14 | 1.77 | | | |
| 0.1 | 2.08 | 1.18 | 1.76 | | | |



FIG. 8. Critical exponents $\kappa$ and $\tau$ determined from the power law fits according to Eq. (17) and Eq. (18). In the case of the exponent $\tau$ the error bars are smaller than the symbols. The scaling equation Eq. (24) holds for $p > 0.6$.

In the limit $p = 1$ the numerical values of the exponents coincide with the exact values [4] $\kappa = \frac{1}{2}$ and $\tau = \frac{1}{3}$.

We should emphasize that the above analysis is not sufficient evidence that the model exhibits SOC for $p \geq 0.5$. To improve the accuracy of the results we analyze the effects due to the finite size of the systems by using simple finite size scaling [6]:

$$P(s, L) = L^{-\beta_s} g(s L^{-\nu_s}). \tag{19}$$

In order that Eq. (18) is recovered for large $L$ the universal function $g(x)$ must obey a power-law behavior for $x \to 0$ and the three exponents $\beta_s$, $\nu_s$, and $\tau$ fulfill the relation

$$\beta_s = \nu_s \tau. \tag{20}$$

The scaling exponent $\nu_s$ can be derived from the fractal dimension $d_\|$: For each value of $p$ we find a cutoff of the

distribution taking place at a size $s_{max}$ which depends on $L$. If finite size scaling works all distributions $P(s, L)$, including their cutoffs, have to collapse, i.e., the argument of the universal function $g$ has to be constant:

$$s_{max} L^{-\nu_s} = \text{const.} \tag{21}$$

On the other hand, we know from Eq. (14) that $\langle s \rangle \langle l_\| \rangle$ scales with the length $l_\|$. Thus $\langle s_{max} \rangle$ scales with $L$ in the same way and both exponents are identical. In this way we have calculated the scaling exponents

$$\beta_s = d_\| \tau \qquad \text{and} \qquad \nu_s = d_\| \tag{22}$$

from the measured exponents $d_\|$ and $\tau$.

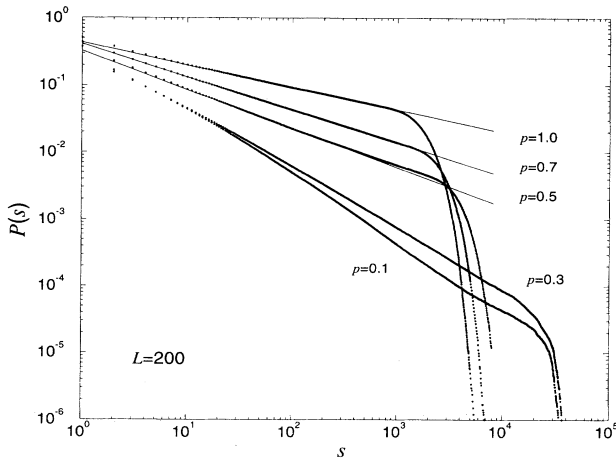In Fig. 9 we show the results of the scaling plot for



FIG. 7. Double logarithmic plot of the probability distribution $P(s)$ of avalanches of size $s$ for various values of $p$ as indicated. The solid lines correspond to power laws.
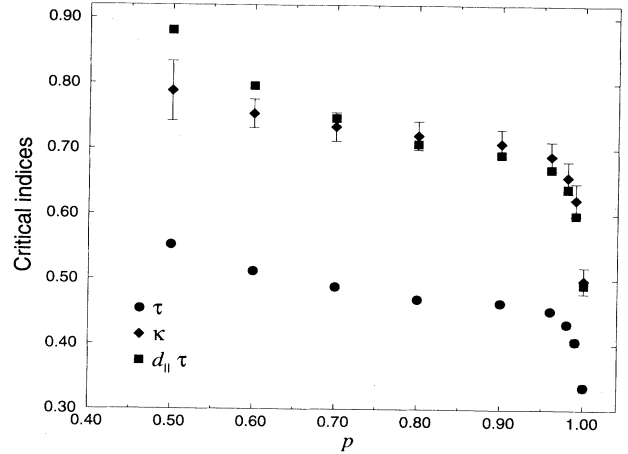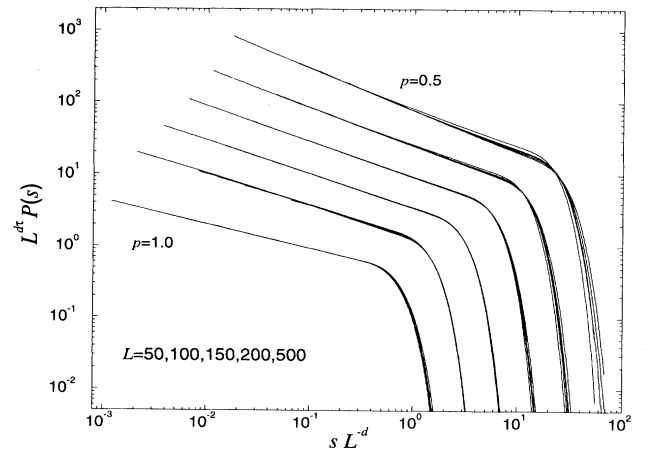


FIG. 9. Finite size scaling analysis of the avalanche size distribution $P(s)$ for $p = 1.0, 0.9, 0.8, 0.7, 0.6$, and 0.5 and five different system sizes $L$. The curves corresponding to $p < 1$ are shifted in the upper right direction. The finite size scaling ansatz works quite well for $p > 0.6$.

$p \geq 0.5$ and five different automata sizes. Finite size scaling works well for $p \geq 0.7$. In the case of $p \leq 0.6$ the deviations grow, i.e., the different curves do not completely collapse.

In the following we will prove a scaling relation among the exponents $\tau$, $\kappa$, and $d_{\parallel}$, indicating that the exponents of the distributions $P(s)$ and $P(l_{\parallel})$ are not independent. The relation

$$p(l_{\parallel}) \, dl_{\parallel} \sim p(l_{\parallel}) \, \frac{dl_{\parallel}}{ds} \, ds \sim p(s) \, ds \qquad (23)$$

and Eq. (14) lead to the scaling relation

$$\kappa = d_{\parallel} \, \tau. \qquad (24)$$

Here $p(l_{\parallel})$ and $p(s)$ represent the probability density of an avalanche of length $l_{\parallel}$ and size $s$, i.e., they obey the power laws $p(l_{\parallel}) \sim l_{\parallel}^{-\kappa-1}$ and $p(s) \sim s^{-\tau-1}$, with $\kappa$ and $\tau$ defined in (17) and (18), respectively.

In Fig. 8 the product $d_{\parallel} \tau$ is also shown and compared with the values of the exponent $\kappa$ for various values of $p$. We conclude that the scaling relation (24) holds for $p \geq 0.7$. These results confirm the finite size scaling analysis and suggest that criticality is lost at a certain point between $p = 0.6$ and $p = 0.7$. We expect that preceding the transition point $p_c$ the occurrence of toppling processes due to the critical slope condition increases and results in a loss of criticality which is connected to the pure critical height behavior.

We have also investigated the avalanche duration $t$ and found that the average duration scales with the length $l_{\parallel}$ according to

$$\langle t \rangle_{l_{\parallel}} \sim l_{\parallel}^z. \qquad (25)$$

Analogous to the size $s$, the probability distribution of the duration obeys a power-law behavior

$$P(t) \sim t^{-\theta} \qquad (26)$$

for $p \geq 0.7$. In the same area of $p$ finite size scaling works quite well and the corresponding scaling relation $\kappa = z\theta$ is fulfilled. The obtained values of the exponents $\theta$ and $z$ are listed in Table I. These measurements confirm our previous conclusion that the system exhibits SOC for $p \geq 0.7$ and not in the whole critical height regime.

## VI. CONCLUSIONS

We have studied numerically a sandpile model with stochastic dynamics which exhibits a nonequilibrium phase transition as the parameter $p$ (representing static friction) is varied. The probability parameter allows us to tune the dynamics from a critical height to a critical slope behavior. The average net slope $\langle \sigma \rangle$ plays the role
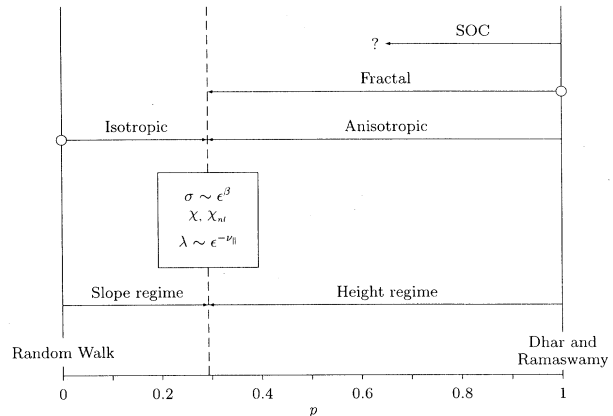


FIG. 10. Phase diagram of the model which illustrates the major properties of the investigated system. The order parameter $\sigma$ and the penetration depth $\lambda$ depend on $\epsilon = |p - p_c|$.

of the order parameter and obeys a power-law dependence in $p_c - p$. In contrast to the diverging penetration depth both the linear and nonlinear susceptibility show no singular behavior on approaching the transition point $p_c$.

We found that the nonequilibrium phase transition is accompanied by a transition from an anisotropic to an isotropic behavior of the avalanches. Fractality occurs only in the case of anisotropic shape of the avalanches.

Finite size scaling analysis works for the probability distributions of the avalanches and scaling relations hold for $p \geq 0.7$, indicating that the system exhibits SOC in this region. The corresponding exponents have a nonuniversal i.e., $p$-dependent, behavior.

Due to long computation time, we did not simulate lattices larger than $L = 500$ in order to check if the power-law behavior is still maintained for values of $p < 0.6$. The problem of disappearance of the SOC on approaching the nonequilibrium phase transition remains for future study.

A complete illustration of the behavior of our sandpile model is depicted in Fig. 10.

## ACKNOWLEDGMENTS

[1] P. Bak, C. Tang, and K. Wiesenfeld, Phys. Rev. Lett. **59**, 381 (1987); Phys. Rev. A **38**, 364 (1988).

[2] G. Grinstein, in *Scale Invariance, Interfaces and Non-Equilibrium Dynamics*, edited by A. McKane *et al.*, NATO Advanced Study Insitute, Series B: Physics Vol. 344 (Plenum, New York, 1995).

[3] H. Flyvbjerg, in *Scale Invariance, Interfaces and Non-Equilibrium Dynamics*, see [2].

[4] D. Dhar and R. Ramaswamy, Phys. Rev. Lett. **63**, 1659 (1989).

[5] S. S. Manna, Physica A **179**, 249 (1991).

[6] L. P. Kadanoff, S. R. Nagel, L. Wu, and S. M. Zhou, Phys. Rev. A **39**, 6524 (1989).

[7] S. Lübeck and K. D. Usadel, Fractals **1**, 1030 (1993).

[8] S. Lübeck, K. D. Usadel, and B. Tadić, in *Fractal Reviews in the Natural and Applied Sciences*, Proceedings of the Fractal Conference, Marseille, 1995, edited by M. M. Novak (Chapman & Hall, London, 1995).

[9] K. Binder and J.-S. Wang, J. Stat. Phys. **55**, 87 (1989).

[10] W. Kinzel, Ann. Israel Phys. Soc. **5**, 425 (1983).

[11] C. Kaiser and L. Turban, J. Phys. A **27**, L579 (1994).